npj | clean water

www.nature.com/npjcleanwater

ARTICLE OPEN

Check for updates

Metal-organic framework modified hydrophilic polyvinylidene fluoride porous membrane for efficient degerming selective oil/water emulsion separation

Qin Ye[1,4], Jia-Min Xu[1,4], Yi-Jie Zhang[1], Shu-Han Chen[1], Xue-Qing Zhan[1], Wang Ni[1], Lung-Chang Tsai[2], Tao Jiang[1], Ning Ma[1,3]✉ and Fang-Chang Tsai[1,2]✉

Developing a new type of superhydrophilic/underwater superoleophobic oil/water separation membrane with high separation efficiency, high throughput and bacteria separation has essential theoretical and practical significance for treating oily and medical wastewater. This work modified commercial PVDF membranes by knife coating and cross-linking, and PVDF/PVA/LPB/MOF hybrid separation membranes are manufactured. Hydrophilic polyvinyl alcohol (PVA) endows the separation membrane with good hydrophilicity. Lauramidopropyl Betaine (LPB) enhances intermolecular hydrogen bonding and improves the mechanical properties of the membrane. A Metal-organic framework (MOF) with excellent biocompatibility, UiO-66-NH_2, plays a vital role in the separation of bacteria. The results of the morphology and surface chemistry of characterization analysis show that the PVDF/PVA/LPB/MOF hybrid separation membrane exhibits excellent superhydrophilicity (with a contact angle of 2°) and high-water flux (15600 L/m^2h) and high separation efficiency (99%), and the nature of filtering bacteria while separating oil. After modification, the separation efficiency increased from 30% to 99%, showing strong oil stain resistance. Our finding suggests that the new type of super-hydrophilic/underwater superoleophobic oil/water separation membrane has potential value in practical applications.

npj Clean Water (2022)5:23 ; https://doi.org/10.1038/s41545-022-00168-z

INTRODUCTION

With the acceleration of the global industrialization process, environmental pollution has become more serious, and there are more and more non-decomposable oils and bacterial communities[1]. Offshore oil spills, industrial oily wastewater discharge, and domestic sewage discharge incidents have caused severe threats to the ecological environment and human health[2–4]. The treatment of organic medical wastewater is one of the challenges facing human beings. Medical wastewater contains many pathogens such as bacteria, viruses, insect eggs, etc.[5]. Hospital sewage is contaminated with feces, infectious bacteria and viruses, and other pathogenic microorganisms, which will cause greater infectivity[6]. Many organisms and bacterial communities exist in food drainage plants and domestic sewage, which are harmful because bacteria can quickly multiply in wastewater[7]. Therefore, treating sewage containing oil and bacteria has attracted global attention. So far, many methods such as biodegradation[8,9], physical adsorption[10], chemical dispersion[11], and combustion[12] have been applied to water purification. However, most of these methods cannot meet these practical application challenges due to complex procedures, low efficiency, high cost, and secondary pollution[13]. Membrane filtration has attracted much attention because of its advantages, such as no chemical additives, high efficiency, no secondary pollution, low maintenance cost, and easy processing in the treatment of oil/water mixtures[14]. Polymer membrane materials have low price, easy processing, adjustable pore size, and distribution, and therefore show great potential in oil/water separation[15]. Membrane filtration technology, especially ultrafiltration (UF) and low-pressure microfiltration (MF), has the advantages of simple operation, low energy consumption, high separation efficiency, and small footprint. It has been reported by Liao et al. as an effective method for oil/water separation[16]. However, under hydrophobic-lipophilic solid interactions, oil droplets tend to accumulate on the surface of polymer membranes, such as polyethersulfone, polypropylene, and polyvinylidene fluoride (PVDF)[17]. Because the hydrophobic surface has a strong affinity for oil droplets, most polymer UF/MF membranes will suffer severe pollution, resulting in a serious reduction in separation efficiency and water flux[18]. Therefore, developing a new polymer membrane with excellent oil stain resistance for oil/water separation is crucial.

Inspired by the oleophobicity of fish scales underwater, materials with super-hydrophilic/underwater oleophobic properties are called "water-removing" materials[19–21]. This material can overcome the disadvantages of secondary pollution of the membrane and adhesion of oil on the surface of the membrane, resulting in a reduction in separation efficiency and water flux[22]. A super-hydrophilic membrane with high hydrophilicity can form a water layer, which acts as an elastic and soft underlayer to prevent oil from directly contacting the membrane surface, resulting in excellent oil/water separation performance and oil stain resistance[23,24]. Huang et al. used atomic layer deposition technology to modify a layer of inorganic nanoparticles on the surface to enhance the super-hydrophilicity of the material. However, this usually requires complicated process conditions such as high temperature and low pressure[25,26]. Through chemical graft

[1]Hubei Key Laboratory of Polymer Materials, Key Laboratory for the Green Preparation and Application of Functional Materials (Ministry of Education), Hubei Collaborative Innovation Center for Advanced Organic Chemical Materials, School of Materials Science and Engineering, Hubei University, Wuhan 430062, China. [2]Hubei Key Laboratory of Economic Forest Germplasm Improvement and Resources Comprehensive Utilization, Hubei Collaborative Innovation Center for the Characteristic Resources Exploitation of Dabie Mountains, Huanggang Normal University, Huanggang 438000, China. [3]State Key Laboratory of Biocatalysis and Enzyme Engineering, School of Life Sciences, Hubei University, Wuhan 430062, China. [4]These authors contributed equally: Qin Ye, Jia-Min Xu. ✉email: ningma@hubu.edu.cn; tfc0323@gmail.com

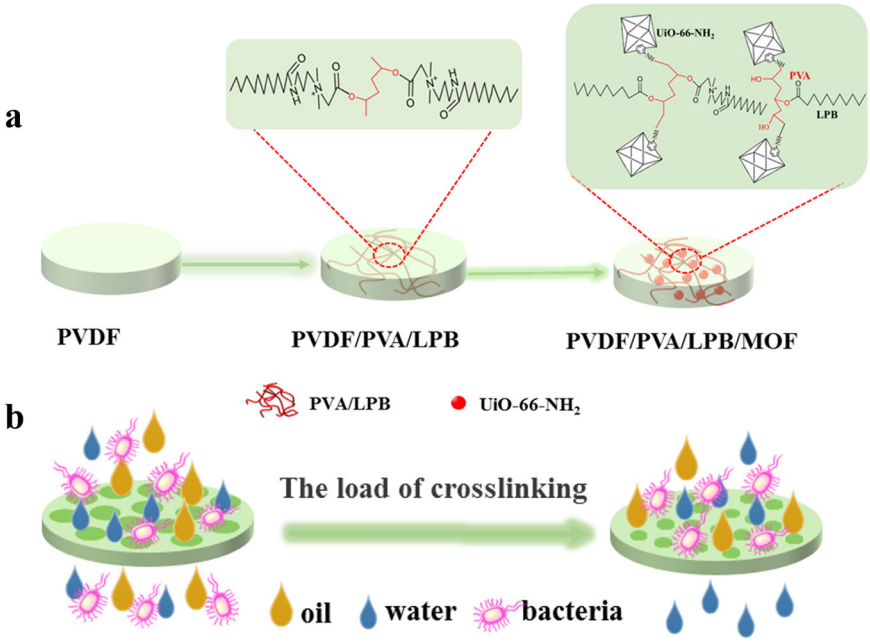

Fig. 1 Schematic diagram of PVDF/PVA/LPB/UiO-66-NH hybrid separation membrane. a Preparation process of PVDF/PVA/LPB/MOF membrane. **b** Degerming and selective oil/water emulsion separation mechanism of PVDF/PVA/LPB/MOF membrane.

modification, more chemical groups are introduced on the surface of the membrane, which can improve the hydrophilicity of the membrane. However, too many chemical groups may lack stability in harsh environments containing acids and alkalis. They will cause the pore size of the membrane to decrease and the water flux to decrease[15,27,28]. Using rigid materials such as stainless steel as the base material lacks deformability and toughness[29]. The use of hydrogel materials may result in weaker mechanical properties[30]. He et al. introduced hydrophilic groups on the surface of the PVDF membrane through a chemical treatment process and then covalently bonded with titanium dioxide nanoparticles and polyvinyl alcohol to construct a coating[31]. However, the entire modification process is cumbersome and complicated and is not conducive to large-scale production.

Polyvinyl alcohol (PVA) is a natural degradable hydrophilic polymer with abundant hydroxyl groups and flexible chains that are easy to extend and have strong chemical stability and film-forming ability[32]. PVA forms a hydrophilic layer on the surface of the PVDF membrane, and the hydrophilic layer gives the membrane good hydrophilicity. There is a covalent bond between PVA and PVDF membrane, making PVDF modified membrane durable[17]. Lauroamidopropyl betaine (LPB) is a quaternary ammonium salt. The carboxylate, amide carbonyl and positively charged amine groups on the surface can form a polymer network through hydrogen bonding with the hydroxyl group of PVA. Thereby improving the mechanical properties of the membrane[32]. Metal-organic framework (MOF) is a porous coordination polymer with high specific surface area, structure, and composition stability and has been widely used[33]. Zirconium-based adsorbents, such as amorphous zirconia nanoparticles, show a strong affinity for pollutants in water and contain zirconium-based porous crystal materials. Active adsorption sites and larger physical contact areas can better absorb some contaminants in the water body[34–36].

In this paper, the knife coating and cross-linking method are used to modify the commercial PVDF membrane, as shown in Fig. 1, the Schematic diagram of PVDF/PVA/LPB/MOF hybrid separation membrane. Cross-linking (curing in situ) on the surface of the original PVDF film enhances the stability of the film[37]. A covalent bond is formed between PVA and PVDF, and the PVA chain is on the PVDF skeleton to form a hydrophilic layer on the surface of the membrane, giving the modified membrane strong hydrophilicity, underwater oleophobicity, and antifouling properties. The separation membrane has excellent stability and shows strong hydrophilicity at different pH values. Mechanical properties are essential in the practical application of membrane materials. The carboxylate, amide carbonyl, and positively charged amine groups on the surface of LPB can form a polymer network through hydrogen bonding with the hydroxyl functional groups of PVA to improve the mechanical properties. The hydrophilic functional groups on the surface of the hybrid separation membrane can interact with surrounding water molecules through hydrogen bonding to form an interface hydration layer on the membrane surface[38,39]. The interface hydration layer can be used as an energy barrier to prevent oil droplets from adhering to the separation membrane and enhance the antifouling performance of the membrane[40]. UiO-66-NH_2 is a porous material with high porosity, a large specific surface area, and is controllable. It has broad application prospects in the treatment of water pollution[41]. Due to the hydrogen bond and polymer network, the amino group of UiO-66-NH_2 can be connected to the surface of the membrane to improve the resistance of the separation membrane, chemical attack ability, and resistance to mechanical damage[42]. UiO-66-NH_2 has a strong positive charge. Electrostatic action can adsorb some negatively charged bacteria by adjusting the pore size of the separation membrane to be smaller than the bacteria and constructing a super-hydrophilic membrane surface to repel/block some bacterial contaminants the microbial and bacterial communities in the wastewater can be integrated. Mei et al. reported this method[43]. Oil and bacteria often coexist in domestic and industrial wastewater. Previous studies have mainly focused on oil/water mixtures, and few studies have involved complex oil/water/bacteria systems. Therefore, the PVDF/PVA/LPB/MOF hybrid separation membrane synthesized in this paper has potential value in useful applications such as offshore oil spills, food processing drainage plants, medical wastewater, and future industrial wastewater, which will have practical and scientific significance.

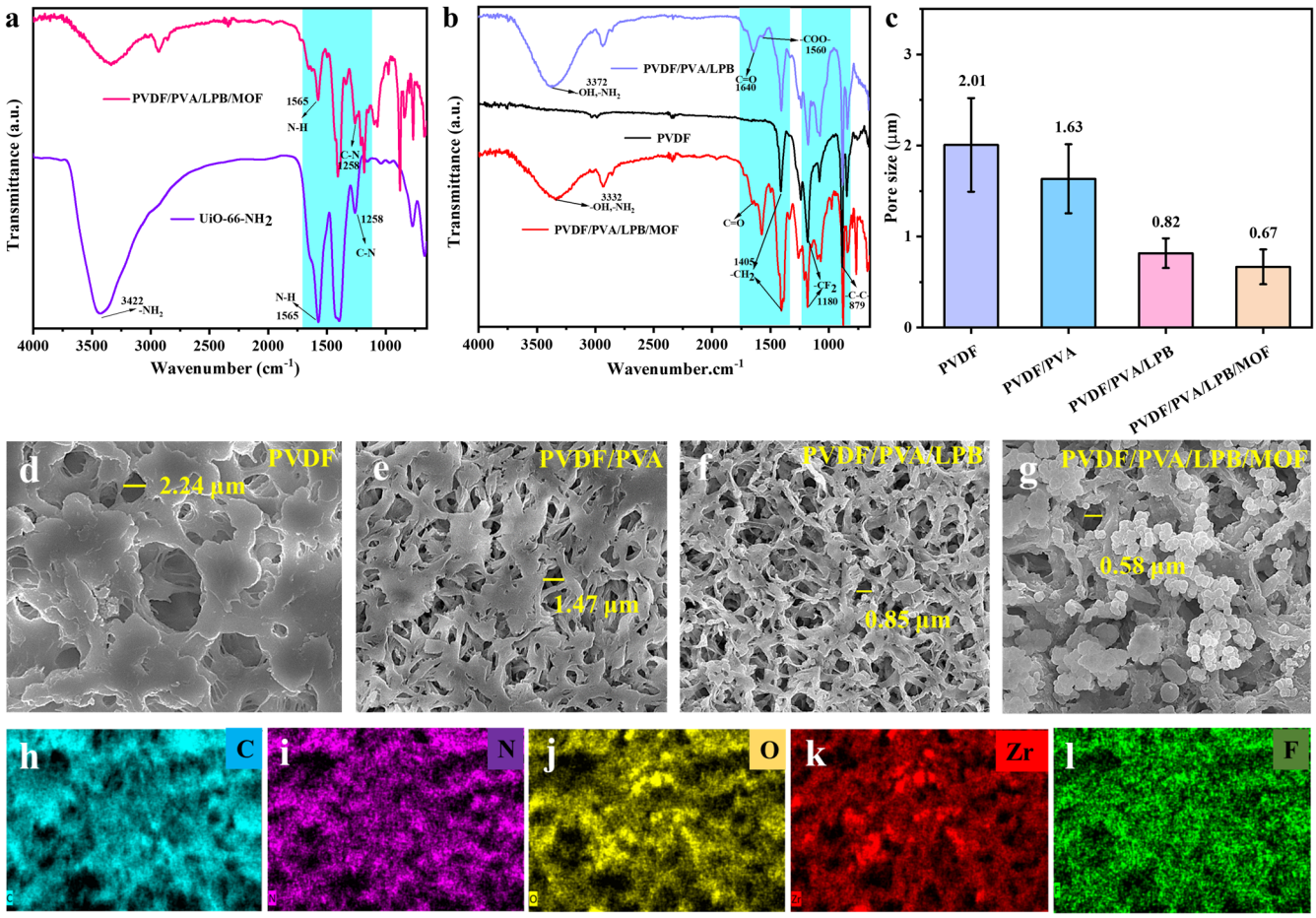

Fig. 2 FT-IR, pore size, and surface morphology of different composite membranes and EDS characterization of PVDF/PVA/LPB/MOF membranes. FTIR spectra of **a** UiO-66-NH_2, PVDF/PVA/LPB/MOF and **b** PVDF/PVA/LPB /MOF, PVDF/PVA/LPB and PVDF membranes. **c** The average pore size of different membranes (s.d.). The FE-SEM images of **d** PVDF, **e** PVDF/PVA, **f** PVDF/PVA/LPB and **g** PVDF/PVA/LPB/MOF membranes (scale bar: 2 μm). EDS elemental mapping of PVDF/PVA /LPB/MOF membranes **h** Carbon, **i** Nitrogen, **j** Oxygen, **k** Zirconium and **l** Fluorine (scale bar: 2 μm).

RESULTS AND DISCUSSION

Characterization of PVDF/PVA/LPB/MOF membranes

Figure 2a, b show the FTTR spectra of UiO-66-NH_2, PVDF/PVA/LPB/MOF, PVDF and PVDF/PVA/LPB. In the UiO-66-NH_2 spectrum, 3422 cm^{-1} is the characteristic peak of $-NH_2$, and 1565 cm^{-1} is the stretching vibration of N-H. 1258 cm^{-1} is the stretching vibration of C-N, which indicates that UiO-66-NH_2 has been successfully synthesized. In the PVDF/PVA/LPB/MOF spectrum, there are characteristic peaks at 1565 cm^{-1} and 1258 cm^{-1}. In addition, 1405 cm^{-1}, 1180 cm^{-1}, and 879 cm^{-1} are stretching vibrations of $-CH_2$, $-CF_2$, $-C-C-$, respectively, which are characteristic peaks of PVDF membranes. In the PVDF/PVA/LPB spectrum, 3372 cm^{-1} is the characteristic peak of $-OH$, $-NH_2$. 1640 cm^{-1} is the characteristic peak of the stretching vibration of the carbonyl group (C=O) of the amido compound of LPB. 1560 cm^{-1} is the characteristic peak of LPB carboxylate ($-COO^-$). The results show that PVDF/PVA/LPB/MOF has been successfully synthesized. Figure 2c show the average pore size of different hybrid membranes. The pore size of the composite membranes was measured by Scale Statistics software (Nano Measurer v1.2), and the pore size distribution map data for each membrane was given. The average pore size of PVDF membrane is 2.01 μm, PVDF/PVA membrane is 1.63 μm, PVDF/PVA/LPB membrane is 0.82 μm and PVDF/PVA/LPB/MOF membrane is 0.67 μm. Figure 2d–g shows the FE-SEM pictures of the surface of PVDF, PVDF/PVA, PVDF/PVA/LPB, and PVDF/PVA/LPB/MOF membranes. The surface morphology of the original PVDF membrane has a highly porous structure. After the modification of PVA, the pore size of the membrane surface is significantly reduced[17]. After the addition of LPB, the membrane surface becomes rougher. The interaction between -OH and -$CONH_2$ in PVA increases the density of the film and improves the toughness. It can be seen from the FE-SEM photo of PVDF/PVA/LPB/MOF hybrid film. The UiO-66-NH_2 particles are supported on the surface of the membrane and remain porous. Figure 2h–l is the EDS of PVDF/PVA/LPB/MOF film. The mixed film contains C, N, O, Zr, and F elements through surface distribution analysis, which shows that PVDF/PVA/LPB/MOF hybrid film has been successfully prepared.

Mechanical and hydrophilic performance of the membranes

As shown in Fig. 3a, the stress-strain curves of different hybrid membranes are shown. With the addition of PVA, LPB, and MOF, the tensile strength of the hybrid membranes tends to increase (Fig. 3b). The PVA chain is easy to extend and has an inherent toughening mechanism[32]. There is a covalent bond between PVDF and PVA film, making the PVA layer on the hybrid film have excellent mechanical durability[17]. Due to the addition of LPB, the interaction among several functional groups $-OH$, $-NH_2$, $-CONH_2$, $-COO-$, formed a polymer network structure based on hydrogen bonds. MOF is a kind of porous polymer, which is well dispersed in the polymer network, making the interaction

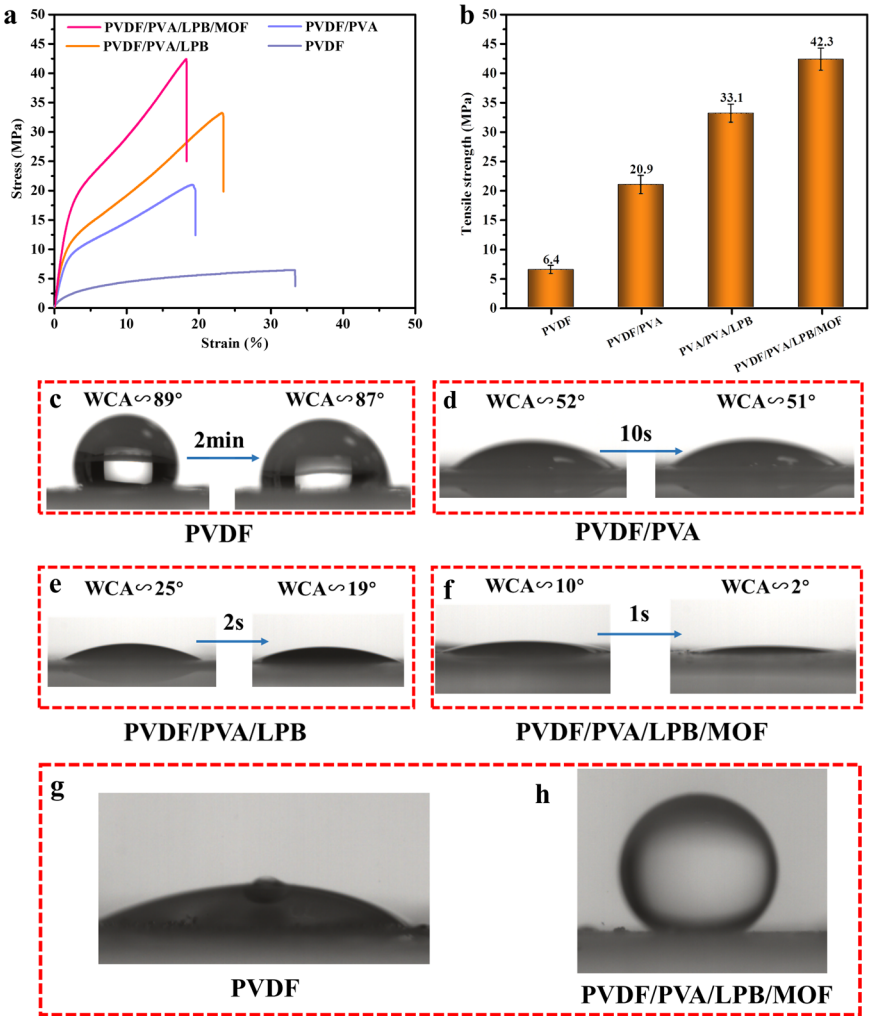

Fig. 3 Mechanical properties and hydrophilicity of different composite films. a The stress-strain diagram of different hybrid membranes. **b** The tensile strength of different hybrid membranes. The change of contact angle (WCA) of **c** PVDF (s.d.), **d** PVDF/PVA, **e** PVDF/PVA/LPB and **f** PVDF/PVA/LPB/MOF film in different time. Underwater oleophobicity of **g** PVDF and **h** PVDF/PVA/LPB/MOF membranes.

between molecules tight and enhancing the mechanical properties of the film[44,45].

As shown in Fig. 3c–f, the hydrophilicity of the film is evaluated by measuring the contact angle of the film. The hydrophilic PVA forms a hydrophilic layer on the surface of the film, giving the film good hydrophilicity. The contact angle of the PVDF/PVA hybrid film is 51° (Fig. 3d). The addition of LPB, due to the presence of -$CONH_2$ and -COO- of LPB, the increase of hydrophilic groups and the interaction between more groups (−OH, −COOH, −$CONH_2$) Therefore, the contact angle of PVDF/PVA/LPB is reduced to 19° (Fig. 3e). The contact angle of PVDF/PVA/LPB/MOF is 2° (Fig. 3f), and the hydrophilicity of the film is enhanced. Due to the enhanced intermolecular force, the network structure formed by the high compatibility of multiple polymers enhances the absorption of water molecules. Figure 3 g, h are the underwater oleophobicity diagrams of PVDF and PVDF/PVA/LPB/MOF membranes. Through modification, the PVDF membrane changes from oleophilic to oleophobic. Underwater super oleophobicity can prevent oil droplets from adhering to the surface of the film and improve the antifouling performance of the membrane[46].

Separation performance of oil-in-water emulsions

The super-hydrophilic and superoleophobic properties of PVDF/PVA/LPB/MOF hybrid membranes help to separate oil/water mixtures selectively. Figure 4a, b shows the contact and departure process of underwater oil droplets (n-hexane) on the surface of PVDF membrane and PVDF/PVA/LPB/MOF mixed membrane. When the PVDF membrane is immersed in water, the sprayed oil droplets (n-hexane, dyed red) easily adhere to the surface of the membrane, and the PVDF membrane will float to the liquid surface due to the adhesion of the oil droplets (Fig. 4a). As shown in Movie S1, the oil stain resistance of the PVDF membrane is relatively poor. On the contrary, when the PVDF/PVA/LPB/MOF hybrid membrane is immersed in water, the sprayed oil droplets rebound rapidly from the surface of the hybrid membrane and do not adhere to the surface of the hybrid membrane (Fig. 4b). As shown in Movie S2, it shows that the PVDF/PVA/LPB/MOF hybrid membrane has strong oil stain resistance. Figure 4c shows the actual oil-water separation device. The red solution represents the oil droplets dyed by Sudan Red III, and the blue solution means the aqueous solution-dyed by methine blue. The oil resistance of the separation membrane is mainly determined by the water retention capacity[47]. As shown in Fig. 4d, e, the oil can directly contact the membrane surface on the surface of the original PVDF membrane. After modification, the surface of the PVDF/PVA/LPB/MOF membrane forms a stable water layer, which can play a buffering role to prevent direct contact between the oil and the membrane surface.

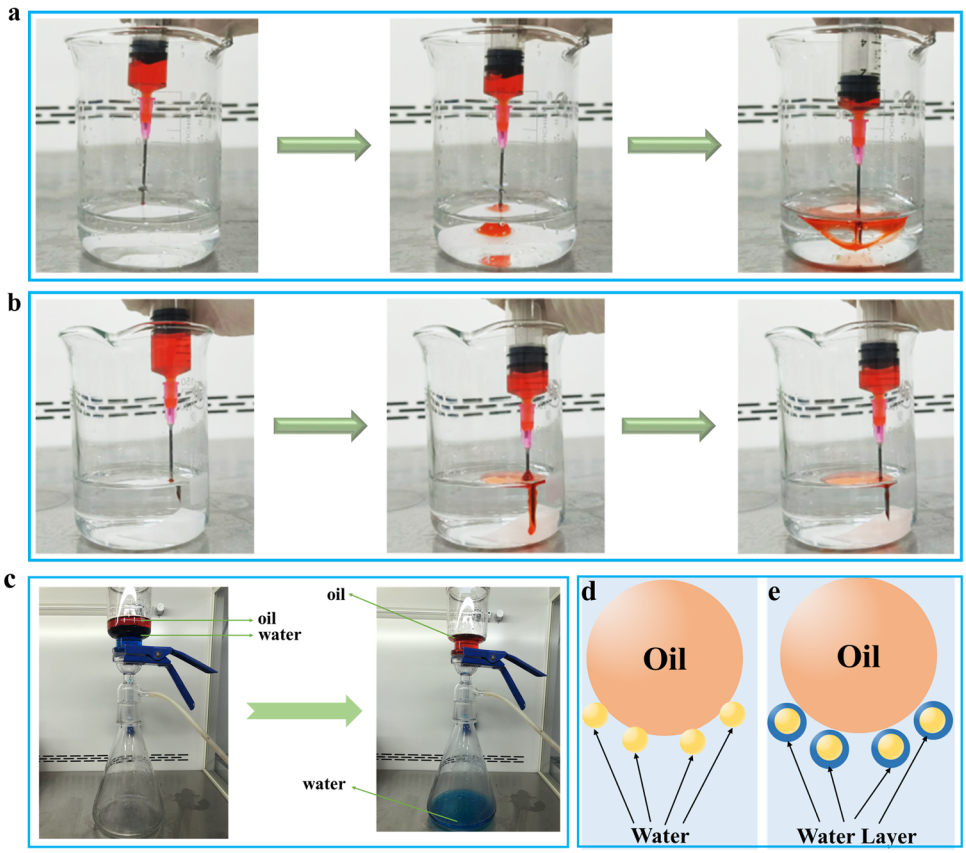

Fig. 4 Oil resistance of PVDF membrane and PVDF/PVA/LPB/MOF membrane. a The anti-oil stain experiment process of PVDF membrane. **b** PVDF/PVA/LPB/MOF membrane anti-greasy experiment process. **c** The device diagram of the oil/water/bacteria separation experiment. Schematic diagram of oil resistance of **d** PVDF and **e** PVDF/PVA/LPB/MOF membranes.

As shown in Fig. 5a–d, there are four O/W emulsions (T/W, S/W, H/W, C/W), the photomicrographs of the feed and filtrate, before and after separation. It can be seen from the figures the collected filtrate (right) is transparent compared to the original milky white emulsion (left). There are still a large number of oil droplets in the feed emulsion. The size of the four oil droplets corresponds to the particle size of Fig. 5e. After the PVDF/PVA/LPB/MOF mixed membrane is filtered, there are almost no oil droplets in the filtrate. It shows that most oil droplets are effectively removed by the composite membrane. Figure 5f shows the water flux and separation efficiency of the PVDF/PVA/LPB/MOF hybrid membrane for four different emulsions. It can be seen that the mixed membrane can effectively eliminate the oil droplets in the emulsion, the water flux can reach more than 15600 L/m^{2}h, and the separation efficiency can reach more than 98.5%. As shown in Fig. 5g, the separation effect of different composite membrane oil/water ($V_{oil}/V_{water} = 1/1$) mixtures shows the water flux (15,650 L m^{-2}h) and separation efficiency of PVDF/PVA/LPB/MOF mixed membranes (90%) are higher than the original PVDF membrane (30%). As shown in Movie S3, the oil/water mixture separates the image. It is proved that most of the oil droplets are effectively removed by the hybrid membrane. On the one hand, it is due to the interaction of PVA and LPB on the surface of the membrane to form a polymer network and reduce the pore size of the membrane. On the other hand, the presence of the hydrophilic layer minimizes the adhesion of surfactant molecules and oil droplets on the surface of the mixed film. Both of these aspects may help improve the water flux and separation efficiency of the PVDF/PVA/LPB/MOF hybrid membrane.

The separation efficiency of the mixed membrane to bacteria

As shown in Fig. 6a–c, it is the FE-SEM membrane of PVDF membrane and PVDF/PVA/LPB/MOF mixed membrane after the bacterial culture solution is filtered. The bacteria filtered out on the membrane surface are far less than those filtered through the PVDF/PVA/LPB/MOF mixed membrane (Fig. 6c). Due to the electrostatic adsorption of UiO-66-NH_2, negatively charged Staphylococcus aureus can be adsorbed. Through the combination of several materials, the pore size of the membrane material gradually decreases, and the pore size of the membrane and the wet membrane surface can block/adsorb bacteria[42]. As shown in Fig. 6d, it can be seen that the bacterial separation efficiency of the PVDF/PVA/LPB/MOF hybrid membrane is higher than that of the original PVDF membrane.

Stability of PVDF/PVA/LPB/MOF membranes

To study the adaptability and durability of the hybrid film in the application process, WCA is tested in different environments. As shown in Fig. 7a, WCA is measured at different pH. Working in strong acid and strong alkaline environments will damage the super-hydrophilicity of the film, while working in other environments has little effect[42]. As shown in Fig. 7b, it can be seen that the super hydrophilicity of the mixed membrane is slightly reduced in different salts, but it can still be maintained at a basic level, and the contact angle is maintained at about 30 °C. It shows that the mixed membrane can be adapted to the separation of offshore petroleum wastewater. As shown in Fig. 7c, different hybrid membranes are placed for different days, and their WCA is measured, and it is found that PVDF/PVA/LPB/MOF have always maintained super-hydrophilic properties. It shows that the hybrid

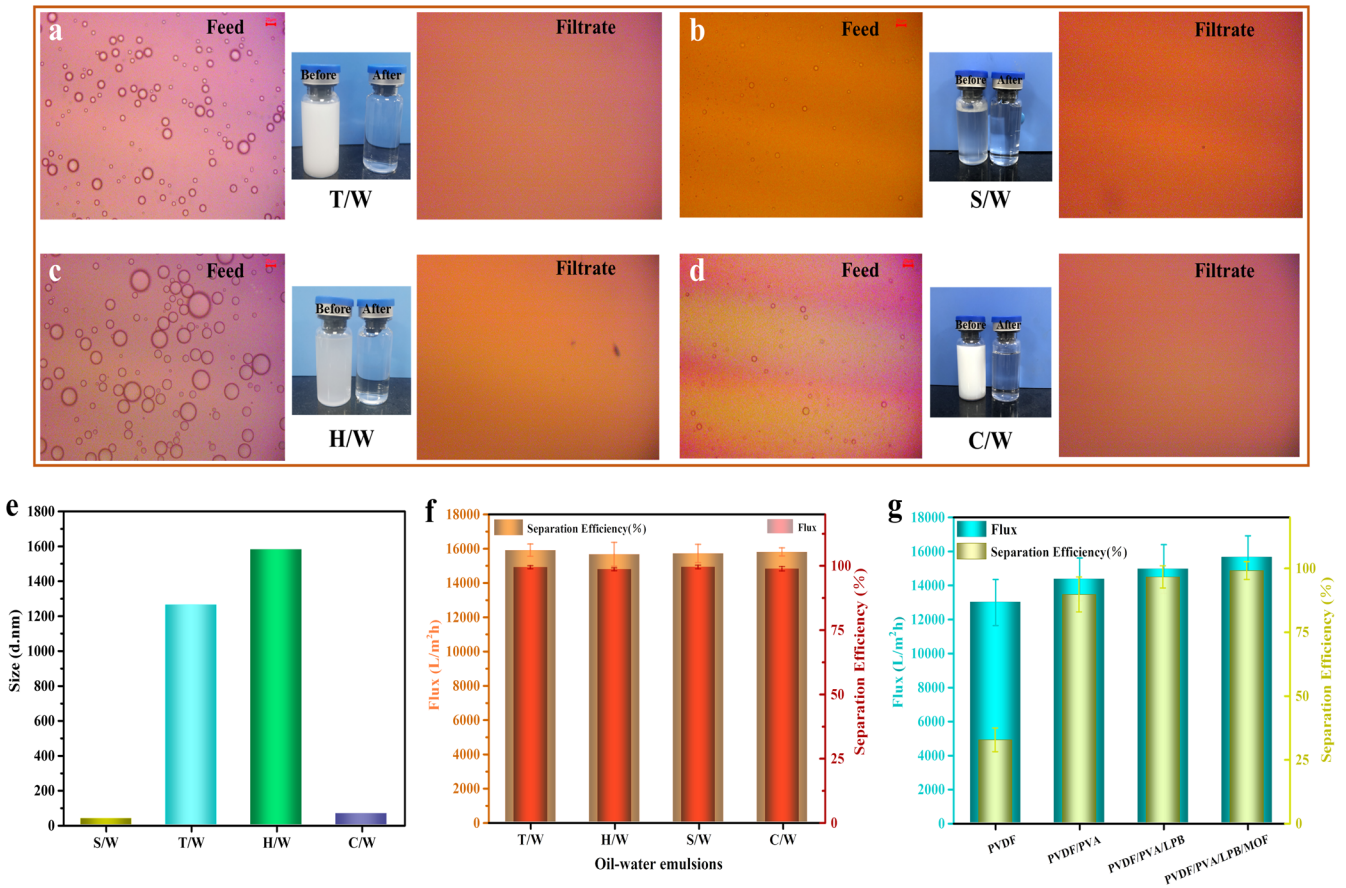

Fig. 5 Separation performance of composite membrane for different stable O/W emulsions. Photomicrographs and images of **a** T/W, **b** S/W, **c** H/W and **d** C/W emulsions before and after PVDF/PVA/LPB/MOF membrane filtration. **e**The particle size of different emulsions. **f** Water flux and separation efficiency of PVDF/PVA/LPB/MOF membrane in different emulsions (s.d.). **g** Water flux and separation efficiency of different mixed membranes in cyclohexane-in-water emulsion (s.d.).

membrane has strong stability and can adapt to different environments.

METHODS

Materials and reagents

PVDF membrane (0.45 μm) purchased from Shanghai Xingya Purification Material Factory (Shanghai, China). Polyvinyl alcohol (PVA) granular powder, its alcoholysis degree is 97.0–98.8%, N, N-dimethylformamide (DMF), acetic acid (HAC), hydrochloric acid (HCl), n-hexane, xylene, petroleum ether, chloroform, Tween 80 and glutaraldehyde (GA) are purchased from Sinopharm Chemical Reagent Co., Ltd. (Shanghai, China). Lauramidopropyl Betaine (LPB) was purchased from Cool Chemical Technology Co., Ltd. (Beijing, China). Sodium chloride (NaCl), magnesium chloride ($MgCl_2$), potassium chloride (KCl), calcium chloride ($CaCl_2$), sodium sulfate (Na_2SO_4) purchased from Sinopharm Chemical Reagent Co., Ltd. (Shanghai, China). Sulfuric acid (H_2SO_4) was bought from Xinyang Chemical Reagent Factory. Sudan Red III was purchased from Tianjin Komeo Chemical Reagent Co., Ltd. Methylene blue was purchased from Tianjin Fuchen Chemical Reagent Factory. Zirconium chloride ($ZrCl_4$) and 2-aminoterephthalic acid are purchased from Aladdin Biochemical Technology Co., Ltd. (Tianjin, China). All materials do not require further purification and can be used directly. Deionized water is manufactured by the laboratory itself.

Synthesis of UiO-66-NH_2

UiO-66-NH_2 is synthesized by the following steps[48], add 0.54 mmol $ZrCl_4$, 5 mL DMF and 0.6 mL HCl into the beaker, mix and sonicate for 30 min. In another beaker, add 0.75 mmol 2-aminoterephthalic acid, 10 mL DMF, and 5 mL HAC, mix and heat in a water bath at 80 °C for 30 min. Then, the two beaker solutions are mixed, poured into a three-necked flask, and react in a microwave at 120 °C for 2 h. The reacted solution is washed three times with DMF and anhydrous ethanol solution, then filtered with suction, and finally dried in an oven at 80 °C for 12 h. UiO-66-NH_2 is finally obtained as a light-yellow powder.

Fabrication of PVDF/PVA/LPB/MOF membranes

As shown in Fig. 8, add 2 g PVA, 2 mL LPB, and 100 mL H_2O into a three-necked flask, and heat and stir at 55 °C for 5 h. The PVDF membrane is soaked in absolute ethanol in advance, washed with deionized water, and dried. Coat the prepared PVA/LPB mixed solution on the PVDF membrane, press it with a glass plate, and brush it three times. Then, it is baked in an oven at 50 °C for 1 h. The film is put into a mixed solution containing 0.5% H_2SO_4 and 1% GA, and cross-linked at 50 °C for 1.5 h. Then, the oven bakes at 50 °C for 15 min to make PVDF/PVA/LPB mixed film. Disperse the pre-prepared UiO-66-NH_2 in an anhydrous ethanol solution, put it into the filter device, and filter it on the PVDF/PVA/LPB composite membrane at 0.04 MPa. Bake in an oven at 50 °C for 1 h, produce a PVDF/PVA/LPB/MOF mixed film.

Instruments and characterization

The group and molecular structure of PVDF/PVA/LPB/MOF film are characterized by Fourier Transform Infrared Spectroscopy (FT-IR) (Nicolet iS 50, Thermo Fisher Scientific). A field emission scanning electron microscope (FE-SEM) (Zeiss Sigma 500, Carl Zeiss, Germany) is used to analyze the surface morphology of the hybrid film. The mechanical properties of the membrane are characterized by the electronic universal tensile testing machine (68TM-10, Shanghai Jiehu Instrument Co., Ltd.), the original gauge length is 20 mm, and the speed is 2 mm/min. The hydrophilicity of the hybrid membrane is characterized by a contact angle measuring instrument (POWEREACH JC2000D1, Shanghai Zhongchen Digital Technology Equipment Co., Ltd.). Observe the images before and

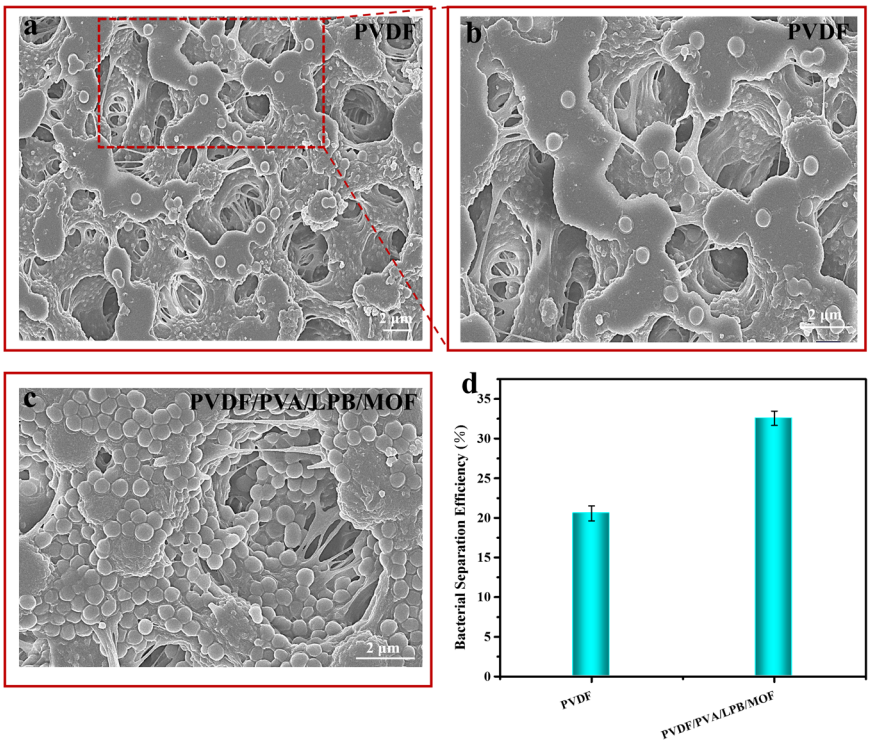

Fig. 6 Isolation of bacteria by PVDF membrane and PVDF/PVA/LPB/MOF membrane. a FE-SEM images after PVDF membrane filtration and **b** further amplified FE-SEM images **c** FE-SEM images after the bacterial solution was filtered by the PVDF/PVA/LPB/MOF membrane. **d** The separation efficiency of PVDF and PVDF/PVA/LPB/MOF membranes for bacteria (s.d.).

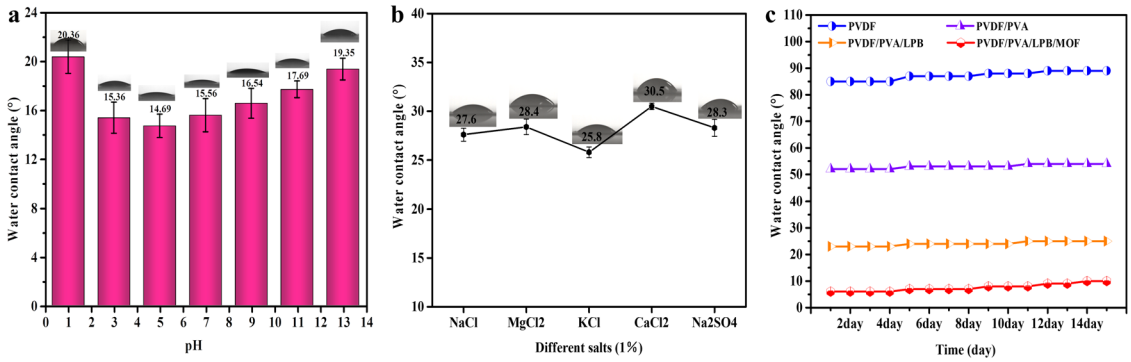

Fig. 7 Environmental stability of different composite films. a The water contact angle (WCA) after PVDF/PVA/LPB/MOF membranes is soaked under different pH conditions (s.d.). **b** WCA of PVDF/PVA/LPB/MOF membrane after immersion in different salt solutions (s.d.). **c** WCA of different mixed membranes placed for different days.

after separation of the oil-in-water O/W emulsion with an Optical microscope (59XF-PC, Beijing Shangguang Instrument Co., Ltd.). The particle size of different oil-in-water O/W emulsions is measured by a nanoparticle size and potential analyzer (Zetasizer Nano ZS90, Derek International Ltd.).

Preparation of oil-in-water emulsions

A surfactant-stabilized oil-in-water emulsion (O/W) is prepared by adding Tween 80 and oil to the water for 30 min under high-shear stirring. For the petroleum ether in water (S/W) emulsion, add 1 g of Tween 80 to 100 mL of water, and then add 4 mL of petroleum ether. For the chloroform-in-water (C/W) emulsion, add 2 g of Tween 80 to 100 mL of water, and then add 1 mL of chloroform. For n-hexane in water (H/W) emulsions, add 1 g of Tween 80 to 100 mL of water, and then add 4 mL of n-hexane. For toluene-in-water (T/W) emulsions, add 0.6 g of Tween 80 to 120 mL of water and 4 mL of toluene. Observed by an optical microscope, the droplet sizes of the obtained emulsions are all in the range of 20 μm.

Oil-in-water emulsions separation

Through the filtering device (Fig. 4c), the mixed membrane is clamped on the sand core of the glass suction filter bottle, and then the oil-in-water emulsion is directly poured into the glass tube and filtered under a pressure of 0.04 MPa. By measuring the amount of permeation within a certain time. Six groups of parallel experiments on one sample. The water flux (F) is calculated by equation[42](1):

$$\text{Flux} = \frac{V}{T \cdot A} \tag{1}$$

Where A is the filtration area of the emulsion (m^2), V is the permeation volume (L), and T is the filtration time (h).

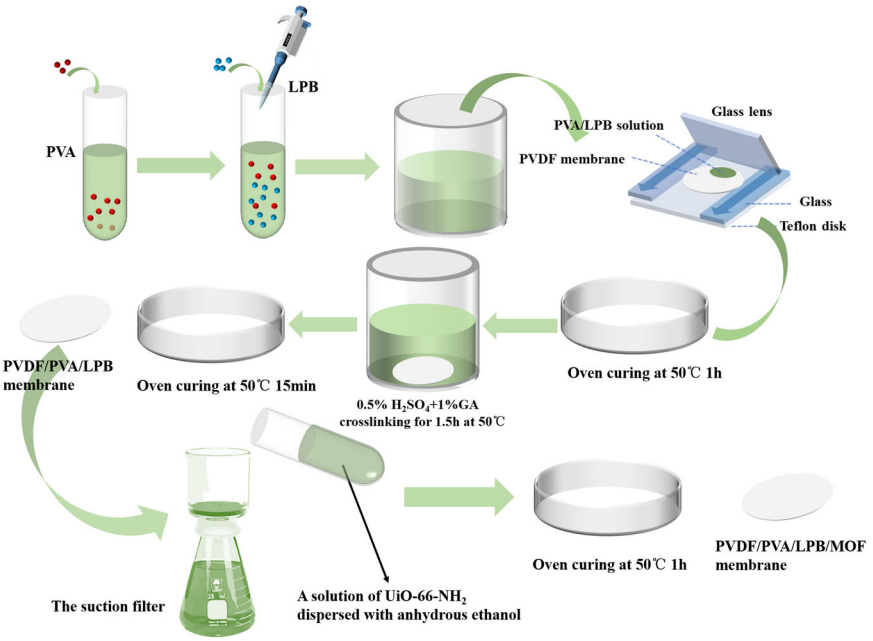

Fig. 8 Synthetic strategy diagram of PVDF/PVA/LPB/UiO-66-NH_2 hybrid separation membrane.

Separate the oil/water mixture under a pressure of 0.04 MPa, clamp the mixed membrane on the sand core of the glass suction flask, and then pour the mixture ($V_{oil}/V_{water} = 1/1$) into the glass tube. Six groups of parallel experiments on one sample. The separation efficiency (S) is calculated by equation[2] (2):

$$S(\%) = \frac{m_1}{m_o} \times 100\% \quad (2)$$

Where m_0 is the mass of water in the original oil-water mixture, and m_1 is the mass of water after filtration.

Hydrophilicity and bacteria separation efficiency measurement

The hydrophilicity of the membrane is evaluated by measuring the water contact angle (WCA) and the interaction of the underwater oil film. We take 5 mL of Staphylococcus aureus (1×10^7 CFU/mL) suspension and pour the bacterial suspension into a glass tube for suction filtration in the form of suction filtration. At a wavelength of 570 nm, using a microplate reader (Bio Tek, ELX800, USA) to measure the optical density (OD) of the filtrate before and after filtration. Six groups of parallel experiments on a sample, the bacteria separation efficiency (S) is calculated by equation[49] (3):

$$S(\%) = \frac{OD_o - OD_1}{OD_0} \times 100\% \quad (3)$$

OD_0 is the optical density value of the bacterial culture solution before filtration, and OD_1 is the visual density value of the filtrate after filtration.

Stability of PVDF/PVA/LPB/MOF membranes

To study the adaptability and durability of PVDF/PVA/LPB/MOF hybrid film, WCA in different environments are tested.

pH test: Put the PVDF/PVA/LPB/MOF mixed membrane in an aqueous solution with pH = 1, 3, 5, 7, 9, 11, 13 for 2 h, and then take it out for testing.

Ion corrosion test: Put the PVDF/PVA/LPB/MOF mixed membrane in a 1% NaCl, $MgCl_2$, KCl, $CaCl_2$, $NaSO_4$ salt aqueous solution for 2 h, and then take it out for testing.

Stability test: Put the PVDF/PVA/LPB/MOF mixed film separately for 1–15 days and then measure the WCA.

DATA AVAILABILITY

The data that support the findings of this study are available from the corresponding author upon reasonable request.

Received: 1 February 2022; Accepted: 27 May 2022;
Published online: 21 June 2022

REFERENCES

1. Dickhout, J. M., Moreno, J., Biesheuvel, P. M., Boels, L. & Lammertink, R. Produced water treatment by membranes: A review from a colloidal perspective. *J. Colloid Interface Sci.* **487**, 523–534 (2017).
2. Zhang, X. et al. Superhydrophobic cellulose acetate/multiwalled carbon nanotube monolith with fiber cluster network for selective oil/water separation. *Carbohydr. Polym.* **259**, 117750 (2021).
3. Fu, S., Chang, Z., Luo, L. & Deng, J. Therapeutic progress and knowledge basis about natriuretic peptide system in heart failure. *Curr. Trends Med. Chem.* **19**, 1850–1866 (2019).
4. Pmga, B., Mn, A., Xw, A. & Bk, B. Silk fibres exhibiting biodegradability & superhydrophobicity for recovery of petroleum oils from oily wastewater—ScienceDirect. *J. Hazard. Mater.* **389**, 121823 (2019).
5. Isık, T. & Demir, M. M. Medical waste treatment via waste electrospinning of PS. *Fibers Polym.* **19**, 767–774 (2018).
6. Lee, S., Kim, Y., Park, J., Shon, H. K. & Hong, S. Treatment of medical radioactive liquid waste using Forward Osmosis (FO) membrane process. *J. Membr. Sci.* **556**, 238–247 (2018).
7. Zhang, P. et al. High throughput of clean water excluding ions, organic media, and bacteria from defect-abundant graphene aerogel under sunlight. *Nano Energy* **46**, 415–422 (2018).
8. Yin, L. et al. Synthesis of layered titanate nanowires at low temperature and their application in efficient removal of U(VI). *Environ. Pollut.* **226**, 125–134 (2017).
9. Wang, J. et al. Catalytic PVDF membrane for continuous reduction and separation of p-nitrophenol and methylene blue in emulsified oil solution. *Chem. Eng. J.* **334**, 579–586 (2018).
10. Zhang, X., Li, Z., Liu, K. & Jiang, L. Bioinspired multifunctional foam with self-cleaning and oil/water separation. *Adv. Funct. Mater.* **23**, 2881–2886 (2013).
11. Al-Sabagh, A. M., Azzam, E. M. S. & El-Din, M. R. N. Synthesis and evaluation of ethoxylated alkyl sulfosuccinates as oil spill dispersants. *J. Dispers. Sci. Technol.* **29**, 866–872 (2008).
12. Shi, X. et al. Influence of ullage to cavity size ratio on in-situ burning of oil spills in ice-infested water. *Cold Reg. Sci. Technol.* **140**, 5–13 (2017).
13. Zhu, X. et al. A versatile approach to produce superhydrophobic materials used for oil–water separation. *J. Colloid Interface Sci.* **432**, 105–108 (2014).
14. Tanudjaja, H. J., Hejase, C. A., Tarabara, V. V., Fane, A. G. & Chew, J. W. Membrane-based separation for oily wastewater: A practical perspective. *Water Res.* **156**, 347–365 (2019).

15. Zhu, Y. et al. Zwitterionic nanohydrogel grafted PVDF membranes with comprehensive antifouling property and superior cycle stability for oil-in-water emulsion separation. *Adv. Funct. Mater.* **28**, 1804121 (2018).
16. Liao, Y., Tian, M. & Wang, R. A high-performance and robust membrane with switchable super-wettability for oil/water separation under ultralow pressure. *J. Membr. Sci.* **543**, 123–132 (2017).
17. Gu, Y. et al. Poly (vinyl alcohol) modification of poly(vinylidene fluoride) microfiltration membranes for oil/water emulsion separation via an unconventional radiation method. *J. Membr. Sci.* **619**, 118792 (2021).
18. Guo, X. et al. G-CNTs/PVDF mixed matrix membranes with improved antifouling properties and filtration performance. *Front. Environ. Sci. Eng.* **6**, 23–33 (2019).
19. Zhang, J. et al. Electrospun flexible nanofibrous membranes for oil/water separation. *J. Mater. Chem. A* **7**, 20075–20102 (2019).
20. Gao, H., Peng, S., Yu, Z., Zeng, X. & Wu, J. A two-step hydrophobic fabrication of melamine sponge for oil absorption and oil/water separation. *Surf. Coat. Technol.* **339**, 147–154 (2018).
21. Wang, Z. et al. Tannic acid encountering ovalbumin: a green and mild strategy for superhydrophilic and underwater superoleophobic modification of various hydrophobic membranes for oil/water separation. *J. Mater. Chem. A* **6**, 13959–13967 (2018).
22. Zhang, Y., Wang, H., Wang, X., Liu, B. & Wei, Y. An anti-oil-fouling and robust superhydrophilic MnCo2O4 coated stainless steel mesh for ultrafast oil/water mixtures separation. *Sep. Purif. Technol.* **264**, 118435 (2021).
23. Zhang, J. et al. Antifouling hydrolyzed polyacrylonitrile/graphene oxide membrane with spindle-knotted structure for highly effective separation of oil-water emulsion. *J. Membr. Sci.* **532**, 38–46 (2017).
24. Li, H. et al. A hierarchical structured steel mesh decorated with metal organic framework/graphene oxide for high-efficient oil/water separation. *J. Hazard. Mater.* **373**, 725–732 (2019).
25. Dong, L. & Zhao, Y. CO_2-switchable membranes: structures, functions, and separation applications in aqueous medium. *J. Mater. Chem. A* **8**, 33 (2020).
26. Huang, A., Kan, C.-C., Lo, S.-C., Chen, L.-H. & Tung, K.-L. Nanoarchitectured design of porous ZnO@copper membranes enabled by atomic-layer-deposition for oil/water separation. *J. Membr. Sci.* **582**, 120–131 (2019).
27. Mi, H. Y., Jing, X., Huang, H. X. & Turng, L. S. Controlling superwettability by microstructure and surface energy manipulation on three dimensional substrates for versatile gravity driven oil/water separation. *ACS Appl. Mater. Interfaces* **9**, 37529–37535 (2017).
28. Liao, Z., Wu, G., Lee, D. & Yang, S. Ultrastable underwater anti-oil fouling coatings from spray assemblies of polyelectrolyte grafted silica nanochains. *ACS Appl. Mater. Interfaces* **11**, 13642–136551 (2019).
29. He, B.-Q. et al. A rubber-like, underwater superoleophobic hydrogel for efficient oil/water separation. *Chem. Eng. J.* **361**, 364–372 (2018).
30. Gao, S. et al. A robust polyionized hydrogel with an unprecedented underwater anti-crude-oil-adhesion property. *Adv. Mater.* **28**, 5307–5314 (2016).
31. Qin, A., Li, X., Zhao, X., Liu, D. & He, C. Engineering a highly hydrophilic PVDF membrane via binding TiO_2 nanoparticles and a PVA layer onto a membrane surface. *ACS Appl. Mater. Interfaces* **7**, 8427–8436 (2015).
32. Ye, Q. et al. Chitosan/polyvinyl alcohol/ lauramidopropyl betaine/2D-HOF mixed film with abundant hydrogen bonds acts as high mechanical strength artificial skin. *Macromol. Biosci.* **20**, e2100317 (2021).
33. Liu, C. et al. Multifunctional CNTs-PAA/MIL101(Fe)@Pt composite membrane for high-throughput oily wastewater remediation. *J. Hazard Mater.* **403**, 123547 (2021).
34. Hang, C., Qi, L., Gao, S. & Jian, K. S. Strong adsorption of arsenic species by amorphous zirconium oxide nanoparticles. *J. Ind. Eng. Chem.* **18**, 1418–1427 (2012).
35. Mahanta, N. & Chen, J.-P. A novel route to the engineering of zirconium immobilized nano-scale carbon for arsenate removal from water. *J. Mater. Chem. A* **1**, 8636–8644 (2013).
36. Wang, C., Liu, X., Chen, J. P. & Li, K. Superior removal of arsenic from water with zirconium metal-organic framework UiO-66. *Sci. Rep.* **5**, 16613 (2015).
37. Wang, D. et al. Antioxidation performance of poly(vinyl alcohol) modified poly (vinylidene fluoride) membranes. *Appl. Surf. Sci.* **435**, 229–236 (2018).
38. He, M. et al. Zwitterionic materials for antifouling membrane surface construction. *Acta Biomater.* **40**, 142–152 (2016).
39. Pin, C., Zhao, S., Chandresh, M. & Wang, R. Polyvinylidene fluoride membrane modification via oxidant-induced dopamine polymerization for sustainable direct-contact membrane distillation. *J. Membr. Sci.* **563**, 31–42 (2018).
40. Guo, D. et al. Fabrication of high-performance composite nanofiltration membranes for dye wastewater treatment: mussel-inspired layer-by-layer self-assembly—ScienceDirect. *J. Colloid Interface Sci.* **560**, 273–283 (2020).
41. Li, X. et al. Water contaminant elimination based on metal–organic frameworks and perspective on their industrial applications. *ACS Sustain. Chem. Eng.* **7**, 4548–4563 (2019).
42. Wang, Y. et al. An integrated strategy for achieving oil-in-water separation, removal, and anti-oil/dye/bacteria-fouling. *Chem. Eng. J.* **413**, 127493 (2021).
43. Mei, L., Ren, Y., Gu, Y., Li, X. & Guo, G. Strengthened and thermally resistant poly (lactic acid) based composite nanofibers prepared via easy stereocomplexation with antibacterial effects. *ACS Appl. Mater. Interfaces* **10**, 42992–43002 (2018).
44. Chen, K., Shi, B., Yue, Y., Qi, J. & Guo, L. J. A. N. Binary synergy strengthening and toughening of bio-inspired nacre-like graphene oxide/sodium alginate composite paper. *ACS Nano* **9**, 8165–8175 (2015).
45. Ye, Q. et al. Chitosan/polyvinyl alcohol/ lauramidopropyl betaine/2D-HOF mixed film with abundant hydrogen bonds acts as high mechanical strength artificial skin. *Macromol. Biosci.* **21**, e2100317 (2021).
46. Zhao, S. et al. An antifouling catechol/chitosan-modified polyvinylidene fluoride membrane for sustainable oil-in-water emulsions separation. *Front. Environ. Sci. Eng.* **4**, 193–203 (2020).
47. Xie, A. et al. Photo-Fenton self-cleaning membranes with robust flux recovery for an efficient oil/water emulsion separation. *J. Mater. Chem. A* **7**, 8491–8502 (2019).
48. Ruan, B. et al. UiO-66 derivate as a fluorescent probe for Fe(3+) detection. *Talanta* **218**, 121207 (2020).
49. Li, M. et al. Highly effective and noninvasive near-infrared eradication of a staphylococcus aureus biofilm on implants by a photoresponsive coating within 20 Min. *Adv. Sci.* **6**, 1900599 (2019).

ACKNOWLEDGEMENTS

This study has been supported by the National Key Research and Development Program of China (SQ2020YFF0413357); Technical Innovation And Development Project of Hubei Province (High-tech Enterprises)(2021BAB085); Supported by Open Funding Project of the State Key Laboratory of Biocatalysis and Enzyme Engineering (SKLBEE2021031); Hubei Provincial Key Laboratory of Economic Forest Germplasm Improvement and Comprehensive Utilization of Resources, Hubei Collaborative Innovation Center for the Characteristic Resources Exploitation of Dabie Mountains, Huanggang Normal University, Huanggang 438000, China (202020504).

AUTHOR CONTRIBUTIONS

F.-C.T.: Supervision, Writing - review & editing, Funding acquisition. N.M.: Substantial contributions to the conception of the work. Q.Y. and J.-M.X.: Synthesis, analysis, and interpretation of the data; Writing—original draft. Y.-J. Z.: FT-IR testing. S.-H.C.: Bacterial isolation. X.-Q.Z.: Methodology. W.N.: Antimicrobial data analysis. T.J.: Final approval of the completed version. L.-C.T.: Revising it critically. Q.Y. and J.-M.X.: contributed equally to this work.

COMPETING INTERESTS

The authors declare no competing interests.

ADDITIONAL INFORMATION

Supplementary information The online version contains supplementary material available at https://doi.org/10.1038/s41545-022-00168-z.

Correspondence and requests for materials should be addressed to Ning Ma or Fang-Chang Tsai.

Reprints and permission information is available at http://www.nature.com/reprints

Publisher's note Springer Nature remains neutral with regard to jurisdictional claims in published maps and institutional affiliations.